

ACCEPTED MANUSCRIPT • OPEN ACCESS

Solving inverse electromagnetic scattering problems via domain derivatives

To cite this article before publication: Felix Hagemann *et al* 2019 *Inverse Problems* in press <https://doi.org/10.1088/1361-6420/ab10cb>

Manuscript version: Accepted Manuscript

Accepted Manuscript is “the version of the article accepted for publication including all changes made as a result of the peer review process, and which may also include the addition to the article by IOP Publishing of a header, an article ID, a cover sheet and/or an ‘Accepted Manuscript’ watermark, but excluding any other editing, typesetting or other changes made by IOP Publishing and/or its licensors”

This Accepted Manuscript is © 2019 IOP Publishing Ltd.

As the Version of Record of this article is going to be / has been published on a gold open access basis under a CC BY 3.0 licence, this Accepted Manuscript is available for reuse under a CC BY 3.0 licence immediately.

Everyone is permitted to use all or part of the original content in this article, provided that they adhere to all the terms of the licence <https://creativecommons.org/licenses/by/3.0>

Although reasonable endeavours have been taken to obtain all necessary permissions from third parties to include their copyrighted content within this article, their full citation and copyright line may not be present in this Accepted Manuscript version. Before using any content from this article, please refer to the Version of Record on IOPscience once published for full citation and copyright details, as permissions may be required. All third party content is fully copyright protected and is not published on a gold open access basis under a CC BY licence, unless that is specifically stated in the figure caption in the Version of Record.

View the [article online](#) for updates and enhancements.

Solving inverse electromagnetic scattering problems via domain derivatives

Felix Hagemann*, Tilo Arens†, Timo Betcke‡, Frank Hettlich§

February 1, 2019

This paper is dedicated to the memory of our friend and colleague Armin Lechleiter.

Abstract

We employ domain derivatives to solve inverse electromagnetic scattering problems for perfect conducting or for penetrable obstacles. Using a variational approach, the derivative of the scattered field with respect to boundary variations is characterized as the solution of a boundary value problem of the same type as the original scattering problem. The inverse scattering problem of reconstructing the scatterer from far field measurements for a single incident field can thus be solved via a regularized iterative Newton scheme. Both the original forward problem and the problem characterizing the domain derivative are formulated as boundary integral equations and we carefully describe how these formulations are obtained in the case of Lipschitz domains. The integral equations are solved using the boundary element library Bempp. A number of numerical examples of shape reconstructions are presented.

1 Introduction

The use of iterative methods based on derivatives with respect to variations of the boundary has been a standard tool for solving inverse problems of shape reconstruction for many years. For many types of boundary value problems characterizations of such shape derivatives have been given, either based on variational approaches or using boundary integral equations, and these characterizations have been employed with great success for computing derivatives in actual implementations of reconstruction algorithms. See e.g. Chapters 4 and 5 in [5] and [10] and the many references given by these authors for an overview on what has been accomplished in this direction, and also [7] for examples of actual reconstructions obtained by this approach in three-dimensional acoustic wave scattering.

*Department of Mathematics, KIT, Karlsruhe, Germany, Email: felix.hagemann@kit.edu

†Department of Mathematics, KIT, Karlsruhe, Germany, Email: tilo.arenas@kit.edu

‡Department of Mathematics, University College London, United Kingdom, Email: t.betcke@ucl.ac.uk

§Department of Mathematics, KIT, Karlsruhe, Germany, Email: frank.hettlich@kit.edu

1
2
3 However, much less has been achieved so far for time-harmonic electromagnetic wave scat-
4 tering problems. The difficulties originate from the much more complicated regularity theory
5 of solutions to Maxwell's equations as compared to solutions of elliptic PDEs. Only in re-
6 cent years have characterizations of shape derivatives been found [6, 9] that are suitable for
7 implementations.
8

9 The situation under consideration in this paper is that of an electromagnetic wave in vacuum
10 being scattered by either a perfectly conducting or penetrable homogeneous obstacle. In this
11 case, the total electromagnetic field is a solution to a boundary value problem consisting of
12 the Maxwell system with constant coefficients, the Silver-Müller radiation condition for the
13 scattered field and a boundary or transmission condition on the boundary of the obstacle. It
14 turns out that the derivative of the far field of the scattered field with respect to variations of
15 the boundary only depends on the *domain derivative* of the scattered field which solves essen-
16 tially the same type of boundary or transmission problem, only with a different inhomogeneity
17 in the boundary or transmission condition. Thus, the domain derivative can be computed by
18 essentially the same numerical methods as the scattered field itself. However, the conditions
19 that characterize the domain derivative involve traces and surface derivative operators that
20 are not implemented in most libraries for computational electromagnetism.
21
22

23 One numerical method that is well suited to the problem type we are considering is the Galerkin
24 boundary element method. The numerical library Bempp (<https://bempp.com>) [16, 17] pro-
25 vides the necessary implementations of boundary element spaces, potentials, integral operators
26 and Calderon-based preconditioners to efficiently solve such scattering problems. Moreover,
27 as we will show below, it is not difficult to implement all the necessary boundary operators for
28 implementing domain derivatives in this framework. Thus, gradient-type iterative methods
29 become a feasible tool to solve inverse electromagnetic scattering problems.
30
31

32 Using these techniques, in this paper we present boundary integral equations of the problems
33 characterizing the domain derivatives and for the first time present an implementation and
34 actual reconstructions of domains using this techniques in full 3D inverse electromagnetic
35 wave scattering. Availability of Bempp has facilitated the implementation of this algorithm
36 tremendously. Nevertheless, the mathematical foundation of the application of boundary
37 integral equations to electromagnetics and the analysis of corresponding boundary element
38 methods is neither elementary nor straight-forward. For the full theory, we refer to [2, 3,
39 4, 14]. We will provide a brief synopsis of those parts of the theory that are vital to the
40 characterization of domain derivatives.
41
42

43 In Section 2, we state the formulation of the direct problems both in variational form and as
44 boundary integral equations. To obtain these formulations, we provide a brief description of
45 how to define the proper Sobolev spaces and boundary differential operators for the Maxwell
46 system. In Section 3, the inverse problem is formulated and gradient based solution schemes
47 are discussed. A boundary integral formulation of the domain derivative of the boundary-
48 to-far-field operator is provided. Details on how to discretize this scheme by choosing an
49 appropriate space of boundary parameterizations are given in Section 4. Section 5 discusses
50 the necessary extensions of the Bempp library to implement the iterative solution algorithm
51 and in Section 6, we provide various numerical examples.
52
53
54
55
56
57
58
59
60

2 Electromagnetic scattering problems and boundary integral formulations

The Maxwell system,

$$\operatorname{curl} E - ikH = 0, \quad \operatorname{curl} H + ikE = 0 \quad (1)$$

with constant wavenumber $k = \omega\sqrt{\varepsilon\mu}$ describes the propagation of time harmonic electromagnetic waves of frequency ω in a linear isotropic homogeneous medium with electric permittivity ε and magnetic permeability μ . In this notation, the time-dependent physical electric field is given by $\mathbf{E}(x, t) = \operatorname{Re}(\varepsilon^{-1/2} E(x) e^{-i\omega t})$ and the magnetic field $\mathbf{H}(x, t) = \operatorname{Im}(\mu^{-1/2} H(x) e^{-i\omega t})$, respectively. Nevertheless, to simplify nomenclature, we will also refer to E as the electric and H as the magnetic field.

Consider a scatterer given by a bounded Lipschitz domain $D \subseteq \mathbb{R}^3$ which may represent either a perfect conducting obstacle or a penetrable inhomogeneity. We assume throughout that $\mathbb{R}^3 \setminus \overline{D}$ is connected. Outside of D , μ and ε are assumed to be equal to the material constants in vacuum, $\varepsilon = \varepsilon_0$, $\mu = \mu_0$.

Consider an incident field (E^i, H^i) which is assumed to be a solution of (1) in all of \mathbb{R}^3 with $k = k_0 = \omega\sqrt{\varepsilon_0\mu_0}$. The presence of the scatterer gives rise to a scattered field E^s, H^s in $\mathbb{R}^3 \setminus \overline{D}$ which is also a solution to (1) and additionally satisfies the Silver-Müller radiation condition

$$\lim_{|x| \rightarrow \infty} [H^s(x) \times x - |x| E^s(x)] = 0. \quad (2)$$

In the case of a perfect conductor, the total field $(E, H) = (E^i, H^i) + (E^s, H^s)$ satisfies the boundary condition

$$E \times \nu = 0 \quad \text{on } \partial D,$$

where ν denotes the outward drawn normal to ∂D . In the case of a penetrable scatterer, we will assume that (ε, μ) are constant in D but different from (ε_0, μ_0) . In addition to (E^s, H^s) , the scatterer gives rise to a transmitted field inside of D which we will also denote by (E, H) . The tangential traces of the physical fields outside and inside of D do not jump across the interface ∂D , which in our notation translates to

$$[\varepsilon^{-1/2} E \times \nu] = 0, \quad [\mu^{-1/2} H \times \nu] = 0 \quad \text{on } \partial D. \quad (3)$$

Throughout this paper, we will consider solutions of these problems in the weak sense. For a Lipschitz domain Ω , we will use the Sobolev space $H(\operatorname{curl}, \Omega)$. Let us briefly outline how the relevant trace and surface differential operators may be defined in this setting. See [2, 3] and the references contained therein for a comprehensive presentation of this subject. For any connected boundary component Γ of Ω , define the tangential trace operators

$$\gamma_t v = v|_{\Gamma} \times \nu, \quad \gamma_T v = \nu \times (v|_{\Gamma} \times \nu), \quad v \in C^\infty(\overline{\Omega}, \mathbb{C}^3),$$

which can be extended continuously to $\gamma_t, \gamma_T : H^1(\Omega, \mathbb{C}^3) \rightarrow L_t^2(\Gamma)$. The range spaces

$$V_t = \gamma_t (H^1(\Omega, \mathbb{C}^3)), \quad V_T = \gamma_T (H^1(\Omega, \mathbb{C}^3)),$$

are in general different from each other. They are Banach spaces with the norms

$$\|\varphi\|_{V_t} = \inf\{\|v\|_{H^1} : \varphi = \gamma_t v\}, \quad \|\psi\|_{V_T} = \inf\{\|v\|_{H^1} : \psi = \gamma_T v\}.$$

Suppose that $u, v \in H^1(\Omega, \mathbb{C}^3)$ vanish outside of a neighborhood of Γ . As a consequence of the divergence theorem, we obtain the integral identity

$$\int_{\Omega} (u \cdot \operatorname{curl} v - \operatorname{curl} u \cdot v) dx = \int_{\Gamma} \gamma_t u \cdot \gamma_T v ds = - \int_{\Gamma} \gamma_T u \cdot \gamma_t v ds. \quad (4)$$

From (4) we can deduce that $\gamma_t : H(\operatorname{curl}, \Omega) \rightarrow V'_T$ and $\gamma_T : H(\operatorname{curl}, \Omega) \rightarrow V'_t$ are bounded with

$$\int_{\Omega} (u \cdot \operatorname{curl} v - \operatorname{curl} u \cdot v) dx = {}_{V'_T} \langle \gamma_t u, \gamma_T v \rangle_{V_T} = {}_{V'_t} \langle \gamma_T u, \gamma_t v \rangle_{V_t} \quad (5)$$

for any $u \in H(\operatorname{curl}, \Omega)$, $v \in H^1(\Omega, \mathbb{C}^3)$ which vanish in a neighborhood of any component of $\partial\Omega$ different from Γ . [2, Proposition 3.4] states that the surface gradient $\nabla_{\Gamma} : H^1(\Gamma) \rightarrow L^2_t(\Gamma)$ maps $W = \{\varphi = v|_{\Gamma} : v \in H^2(\Omega)\}$ to V_T . Thus, the weak definition of the surface divergence as the adjoint of ∇_{Γ} ,

$${}_{H^{-1}(\Gamma)} \langle \operatorname{Div}_{\Gamma} \varphi, \psi \rangle_{H^1(\Gamma)} = - \int_{\Gamma} \varphi \cdot \nabla_{\Gamma} \psi ds, \quad \varphi \in L^2_t(\Gamma), \quad \psi \in H^1(\Gamma), \quad (6)$$

has a well-defined bounded extension $\operatorname{Div}_{\Gamma} : V'_T \rightarrow W'$. Using (5), it turns out that for $u \in H(\operatorname{curl}, \Omega)$, there holds $\operatorname{Div}_{\Gamma}(\gamma_t(u)) \in H^{-1/2}(\Gamma)$ and that the mapping

$$\gamma_t : H(\operatorname{curl}, \Omega) \rightarrow H^{-1/2}(\operatorname{Div}_{\Gamma}, \Gamma) = \{\varphi \in V'_T : \operatorname{Div}_{\Gamma}(\varphi) \in H^{-1/2}(\Gamma)\}$$

is bounded and surjective. In a similar way, the scalar surface curl operator $\operatorname{Curl}_{\Gamma}$ is defined and it is proved that

$$\gamma_T : H(\operatorname{curl}, \Omega) \rightarrow H^{-1/2}(\operatorname{Curl}_{\Gamma}, \Gamma) = \{\varphi \in V'_t : \operatorname{Curl}_{\Gamma}(\varphi) \in H^{-1/2}(\Gamma)\}$$

is also bounded and surjective. It can be shown [2, Lemma 5.6] that the right hand side of (4) extends to a duality $\langle \cdot, \cdot \rangle_{\Gamma}$ between $H^{-1/2}(\operatorname{Div}_{\Gamma}, \Gamma)$ and $H^{-1/2}(\operatorname{Curl}_{\Gamma}, \Gamma)$ such that

$$\langle \gamma_t u, \gamma_T v \rangle_{\Gamma} = \int_{\Omega} (u \cdot \operatorname{curl} v - \operatorname{curl} u \cdot v) dx$$

for all $u, v \in H(\operatorname{curl}, \Omega)$ which vanish in a neighborhood of any component of $\partial\Omega$ different from Γ .

We additionally define the magnetic trace operator $\gamma_N : H(\operatorname{curl}^2, \Omega) \rightarrow H^{-1/2}(\operatorname{Div}_{\Gamma}, \Gamma)$, where

$$\gamma_N v = \frac{1}{ik} \gamma_t \operatorname{curl} v.$$

The term *magnetic* comes from the fact that $\gamma_N v$ is the tangential trace of the magnetic field whenever v is an electric field.

With these tools, we are able to state weak formulations of our scattering problems for the scatterer D . Denote by B an open ball sufficiently large such that $\overline{D} \subseteq B$. On the artificial boundary ∂B , we use the Calderon operator $\Lambda : H^{-1/2}(\operatorname{Div}_{\partial B}, \partial B) \rightarrow H^{-1/2}(\operatorname{Div}_{\partial B}, \partial B)$ that maps the tangential traces on ∂B of a radiating electric field in $\mathbb{R}^3 \setminus \overline{B}$ to the tangential traces of the corresponding magnetic field, $\Lambda \gamma_t E^s = \gamma_N E^s$ (see [14, Section 9.4]).

Define the space

$$V_0 = \{u \in H(\operatorname{curl}, B \setminus \overline{D}) : \gamma_t u = 0 \text{ on } \partial D\}.$$

A weak solution of the perfect conductor problem is a field $E \in V_0$ such that

$$\begin{aligned} \int_{B \setminus \bar{D}} [\operatorname{curl} E \cdot \overline{\operatorname{curl} v} - k_0^2 E \cdot \bar{v}] dx + \langle ik_0 \Lambda \gamma_t E, \gamma_T v \rangle_{\partial B} \\ = \langle ik_0 \Lambda \gamma_t E^i - ik_0 \gamma_N E^i, \gamma_T v \rangle_{\partial B} \quad \text{for all } v \in V_0. \end{aligned} \quad (7)$$

For a penetrable scatterer, we additionally introduce the space

$$W_0 = \{u \in H(\operatorname{curl}, D) : \gamma_t u = 0 \text{ on } \partial D\}.$$

Denote by $\kappa = \omega \sqrt{\varepsilon \mu}$ the wavenumber in D . We look for a field $E \in L^2(B, \mathbb{C}^3)$ such that $E|_D \in H(\operatorname{curl}, D)$, $E|_{B \setminus \bar{D}} \in H(\operatorname{curl}, B \setminus \bar{D})$ with

$$\begin{aligned} \int_{B \setminus \bar{D}} [\operatorname{curl} E \cdot \overline{\operatorname{curl} v} - k_0^2 E \cdot \bar{v}] dx + \langle ik_0 \Lambda \gamma_t E, \gamma_T v \rangle_{\partial B} \\ = \langle ik_0 \Lambda \gamma_t E^i - ik_0 \gamma_N E^i, \gamma_T v \rangle_{\partial B} \quad \text{for all } v \in V_0, \end{aligned} \quad (8a)$$

$$\int_D [\operatorname{curl} E \cdot \overline{\operatorname{curl} v} - \kappa^2 E \cdot \bar{v}] dx = 0 \quad \text{for all } v \in W_0, \quad (8b)$$

together with the transmission conditions (3) on ∂D . Here and in what follows, let superscripts \cdot^+ and \cdot^- indicate traces taken from $\mathbb{R}^3 \setminus \bar{D}$ and D , respectively. Then (3) translates to

$$\varepsilon_0^{-1/2} \gamma_t^+ E = \varepsilon^{-1/2} \gamma_t^- E, \quad \mu_0^{-1/2} \gamma_N^+ E = \mu^{-1/2} \gamma_N^- E. \quad (8c)$$

Solutions to these problems can be computed using boundary integral equations. Our derivation follows the presentation in [4, 12], but see also [5] for a classical derivation for smooth boundaries. For the perfect conductor problem, introduce the *electric potential*

$$\mathcal{E}_k : H^{-1/2}(\operatorname{Div}_{\partial D}, \partial D) \rightarrow H(\operatorname{curl}^2, D)$$

as

$$\mathcal{E}_k \varphi(x) = ik \int_{\partial D} \varphi(y) \Phi_k(x, y) ds(y) - \frac{1}{ik} \operatorname{grad} \int_{\partial D} \operatorname{Div}_{\partial D} \varphi(y) \Phi_k(x, y) ds(y), \quad x \in \mathbb{R}^3 \setminus \partial D,$$

where

$$\Phi_k(x, y) = \frac{e^{ik|x-y|}}{4\pi|x-y|}, \quad x, y \in \mathbb{R}^3, \quad x \neq y,$$

denotes the fundamental solution of the Helmholtz equation. The corresponding *electric boundary operator* $\mathbf{E}_k : H^{-1/2}(\operatorname{Div}_{\partial D}, \partial D) \rightarrow H^{-1/2}(\operatorname{Div}_{\partial D}, \partial D)$ is defined by averaging the traces of the potential from both sides of the boundary,

$$\mathbf{E}_k = \frac{1}{2} (\gamma_t^+ \mathcal{E}_k + \gamma_t^- \mathcal{E}_k).$$

A solution to the perfect conductor problem (7) is then given by $E = E^i - \mathcal{E}_{k_0} \varphi$ if $\varphi \in H^{-1/2}(\operatorname{Div}_{\partial D}, \partial D)$ is a solution to the electric field integral equation (EFIE),

$$\mathbf{E}_{k_0} \varphi = \gamma_t^+ E^i \quad \text{on } \partial D. \quad (9)$$

Note that the EFIE is not uniquely solvable if k_0^2 is an interior electric eigenvalue (cf. [3, Definition 4]). Thus, from here on we will assume that this is not the case.

For the transmission problem, the *magnetic potential* $\mathcal{H}_k : H^{-1/2}(\text{Div}_{\partial D}, \partial D) \rightarrow H(\text{curl}^2, D)$ is required additionally. It is defined as

$$\mathcal{H}_k \varphi(x) = \text{curl} \int_{\partial D} \varphi(y) \Phi_k(x, y) \, ds(y), \quad x \in \mathbb{R}^3 \setminus \partial D,$$

and the corresponding *magnetic boundary operator*

$$\mathbf{H}_k = \frac{1}{2} (\gamma_t^+ \mathcal{H}_k + \gamma_t^- \mathcal{H}_k)$$

The traces of \mathcal{E}_k and \mathcal{H}_k are related to \mathbf{E}_k and \mathbf{H}_k in the following way:

$$\begin{aligned} \gamma_t^\pm \mathcal{E}_k &= \mathbf{E}_k, & \gamma_N^\pm \mathcal{E}_k &= \mp \frac{1}{2} \mathbf{I} + \mathbf{H}_k, \\ \gamma_t^\pm \mathcal{H}_k &= \mp \frac{1}{2} \mathbf{I} + \mathbf{H}_k, & \gamma_N^\pm \mathcal{H}_k &= -\mathbf{E}_k, \end{aligned} \quad (10)$$

where \mathbf{I} denotes the identity operator.

Using the *multitrace operator*

$$\mathbf{A}_k = \begin{bmatrix} \mathbf{H}_k & \mathbf{E}_k \\ -\mathbf{E}_k & \mathbf{H}_k \end{bmatrix},$$

from the Stratton-Chu representation formulas we obtain the equations

$$\begin{bmatrix} \gamma_t^+ E \\ \gamma_N^+ E \end{bmatrix} = \left(\frac{1}{2} \mathbf{I} - \mathbf{A}_{k_0} \right) \begin{bmatrix} \gamma_t^+ E \\ \gamma_N^+ E \end{bmatrix}, \quad \begin{bmatrix} \gamma_t^- E \\ \gamma_N^- E \end{bmatrix} = \left(\frac{1}{2} \mathbf{I} + \mathbf{A}_\kappa \right) \begin{bmatrix} \gamma_t^- E \\ \gamma_N^- E \end{bmatrix}. \quad (11)$$

The operators $\mathbf{C}_k^\pm = \frac{1}{2} \mathbf{I} \mp \mathbf{A}_k$ are called *Calderon projectors* and map pairs of elements in $H^{-1/2}(\text{Div}_{\partial D}, \partial D)$ to admissible Cauchy data of the Maxwell system. We write (8c) as

$$\begin{bmatrix} \gamma_t^+(E^s + E^i) \\ \gamma_N^+(E^s + E^i) \end{bmatrix} = \begin{bmatrix} \varepsilon_r^{-1/2} \mathbf{I} & \mathbf{0} \\ \mathbf{0} & \mu_r^{-1/2} \mathbf{I} \end{bmatrix} \begin{bmatrix} \gamma_t^- E \\ \gamma_N^- E \end{bmatrix} = \mathbf{S} \begin{bmatrix} \gamma_t^- E \\ \gamma_N^- E \end{bmatrix}$$

where $\varepsilon_r = \varepsilon/\varepsilon_0$, $\mu_r = \mu/\mu_0$. The Calderon projectors satisfy

$$\mathbf{C}^+ \begin{bmatrix} \gamma_t^+ E^s \\ \gamma_N^+ E^s \end{bmatrix} = \begin{bmatrix} \gamma_t^+ E^s \\ \gamma_N^+ E^s \end{bmatrix}, \quad \mathbf{C}^- \begin{bmatrix} \gamma_t^- E \\ \gamma_N^- E \end{bmatrix} = \begin{bmatrix} \gamma_t^- E \\ \gamma_N^- E \end{bmatrix},$$

so that

$$\mathbf{S} \mathbf{C}^- \mathbf{S}^{-1} \begin{bmatrix} \gamma_t^+(E^s + E^i) \\ \gamma_N^+(E^s + E^i) \end{bmatrix} = \mathbf{S} \mathbf{C}^- \begin{bmatrix} \gamma_t^- E \\ \gamma_N^- E \end{bmatrix} = \mathbf{C}^+ \begin{bmatrix} \gamma_t^+ E^s \\ \gamma_N^+ E^s \end{bmatrix} + \begin{bmatrix} \gamma_t^+ E^i \\ \gamma_N^+ E^i \end{bmatrix}.$$

This equation can be rewritten as

$$(\mathbf{S} \mathbf{A}_\kappa \mathbf{S}^{-1} + \mathbf{A}_{k_0}) \begin{bmatrix} \gamma_t^+ E^s \\ \gamma_N^+ E^s \end{bmatrix} = \left(\frac{1}{2} \mathbf{I} - \mathbf{S} \mathbf{A}_\kappa \mathbf{S}^{-1} \right) \begin{bmatrix} \gamma_t^+ E^i \\ \gamma_N^+ E^i \end{bmatrix} \quad (12)$$

which is a boundary integral formulation of (8). Theorem 12 in [3] establishes that this equation is uniquely solvable for every incident data pair.

3 Inverse scattering problems and domain derivatives

So far we have discussed formulations of the direct problems of computing the scattered fields from knowledge of the incident field and the shape and physical properties of the scatterer. Now we wish to discuss the inverse problem of reconstructing the shape of the scatterer from knowledge of the incident field and of the scattered field away from the scatterer. We will approach this problem using iterative regularization methods. For this type of methods it is also important to know *a priori* if the scatterer is penetrable or a perfect conductor.

The scattered electric field E^s in $\mathbb{R}^3 \setminus \bar{D}$ satisfies an asymptotic representation

$$E^s(x) = \frac{e^{ik_0|x|}}{4\pi|x|} \left[E_\infty(\hat{x}) + O\left(\frac{1}{|x|}\right) \right], \quad |x| \rightarrow \infty,$$

with $\hat{x} = x/|x|$. E_∞ is called the *electric far field pattern*. It is an analytic tangential vector field on the unit sphere \mathbb{S}^2 , and E_∞ uniquely defines E^s . However, the reconstruction of E^s from E_∞ is a severely ill-posed problem.

We fix an incident field (E^i, H^i) and restrict ourselves to an appropriately chosen class of admissible boundaries \mathcal{Y} . We define the non-linear (electric) *boundary-to-far-field operator*

$$\mathbf{F} : \begin{cases} \mathcal{Y} \longrightarrow L_t^2(\mathbb{S}^2) \\ \partial D \mapsto E_\infty \end{cases}$$

The inverse problem can then concisely be formulated as: given an $E_\infty \in L_t^2(\mathbb{S}^2)$, find $\partial D \in \mathcal{Y}$ that satisfies the equation

$$\mathbf{F}(\partial D) = E_\infty. \quad (13)$$

In order to formulate an iterative solution technique for this non-linear equation, we need to find its linearization. To do this in a mathematically rigorous way requires to formulate variational problems in perturbed domains generated by boundary variations. We consider variations of D , described by sufficiently small $\eta \in C^1(\mathbb{R}^3, \mathbb{R}^3)$, compactly supported in a neighborhood of ∂D such that the diffeomorphism ξ defined by $\xi(x) = x + \eta(x)$ gives a perturbed domain D_η with admissible boundary $\partial D_\eta = \{y = \xi(x) : x \in \partial D\}$. For such variations of D there exists the so called *domain derivative* E' [8, 9], a radiating solution of Maxwell's equations with far field E'_∞ depending linearly on η , such that

$$\frac{1}{\|\eta\|_{C^1(\mathbb{R}^3)}} \|\mathbf{F}(\partial D_\eta) - \mathbf{F}(D) - E'_\infty\|_{L^2(\mathbb{S}^2)} \rightarrow 0, \quad \eta \rightarrow 0. \quad (14)$$

If we choose a certain type of parameterizations \mathcal{Y} in a subset of a normed space \mathcal{X} , for example star like domains, (14) means, that the operator \mathbf{F} possesses a Fréchet derivative for any admissible boundary ∂D with

$$\mathbf{F}'[\partial D] : \mathcal{X} \rightarrow L_t^2(\mathbb{S}^2), \quad \mathbf{F}'[\partial D]\eta = E'_\infty.$$

In order to solve (13), we use a regularized iterative Newton scheme as follows. First, we choose a starting guess ∂D^0 . Every iteration $i \in \mathbb{N}$ consists of the following steps:

- (i) Calculate $\mathbf{F}(\partial D^i)$.

- (ii) Check residual $r = \|\mathbf{F}(\partial D^i) - E_\infty\|$.
- (iii) Solve for $\eta \in \mathcal{X}$ in the linearization of $\mathbf{F}(\partial D_\eta^i) = E_\infty$.
- (iv) Update $\partial D^i \rightarrow \partial D^{i+1}$ by adding η to the parametrization.

We stop the iteration, if the residual r falls below a chosen threshold. The step (iii) needs some further explanation. Assuming that for small η the linearization $\mathbf{F}(\partial D_\eta) \approx \mathbf{F}(\partial D) + \mathbf{F}'[\partial D]\eta$ is a good approximation, we consider the equation

$$\mathbf{F}'[\partial D_i]\eta = E_\infty - \mathbf{F}(\partial D_i). \quad (15)$$

In general we cannot expect (15) to be solvable. However, applying Tikhonov regularization with some regularization parameter $\alpha > 0$, transforms (15) to the uniquely solvable equation

$$(\mathbf{F}'[\partial D_i]^* \mathbf{F}'[\partial D_i] + \alpha \mathbf{I})\eta = \mathbf{F}'[\partial D_i]^*(E_\infty - \mathbf{F}(\partial D_i)). \quad (16)$$

The regularization in (iii) is needed both for solvability of (15) and for damping in (iv) since we need to enforce that the updated boundary is admissible. The identity in the Tikhonov equation (16) corresponds to a penalty with respect to the norm of \mathcal{X} . Stronger norms can be considered, which will be explained below. Consider [11] for details on such iterative regularization schemes and convergence results, which are to our knowledge not known for inverse scattering problems.

The implementation of the algorithm above requires the computation of $\mathbf{F}'[\partial D]$ or, equivalently, of the domain derivative E' . It is possible to characterize the domain derivative via a boundary value problem [8, 9], however, it is necessary to impose additional regularity on the boundary ∂D to do so. Hence, we will from now on assume that D is of class C^1 . Note that this assumption has strong implications for the regularity of the solutions to the scattering problems (7) and (8), respectively: we obtain $E, H \in H^1(D)$, $E^s, H^s \in H^1(B \setminus \overline{D})$ [1] whenever the incident field is smooth enough.

We will briefly outline how domain derivatives can be obtained for electromagnetic scattering problems. We use the approach from [8, 9] via variational methods. Different approaches exist [6, 13, 15]. The case treated in [9] is that of a penetrable scatterer. Introducing the normal trace operator

$$\gamma_\nu v = \nu \cdot v|_{\partial D},$$

we conclude that $\gamma_\nu v \in H^{1/2}(\partial D)$ where v denotes any of the fields E, H, E^s, H^s . By [2, Proposition 3.6], we also have $\nabla_{\partial D}(\eta) \times \nu \in H^{-1/2}(\text{Div}_{\partial D}, \partial D)$ for any $\eta \in H^{1/2}(\partial D)$, as this operator is nothing else than the vectorial surface curl in disguise.

The domain derivative E' depends linearly on a variation of the geometry η . In [9] a characterization of E' as the weak solution of Maxwell's equations with a certain transmission condition is derived. The jumps across ∂D depend on the normal component of η on ∂D , $h = \gamma_\nu \eta \in C^1(\partial D)$. It is proved that E' is a solution of (8a), (8b) with $E^i = 0$ such that the

following transmission conditions are met

$$\begin{aligned}
\varepsilon_0^{-1/2} \gamma_t^+ E' - \varepsilon^{-1/2} \gamma_t^- E' &= \varepsilon_0^{-1/2} \left(-\nabla_{\partial D} (h\gamma_\nu^+ E) \times \nu + ik_0 h \gamma_T^+ H \right) \\
&\quad + \varepsilon^{-1/2} \left(\nabla_{\partial D} (h\gamma_\nu^- E) \times \nu - i\kappa h \gamma_T^- H \right) \\
\mu_0^{-1/2} \gamma_t^+ H' - \mu^{-1/2} \gamma_t^- H' &= \mu_0^{-1/2} \left(-\nabla_{\partial D} (h\gamma_\nu^+ H) \times \nu - ik_0 h \gamma_T^+ E \right) \\
&\quad + \mu^{-1/2} \left(\nabla_{\partial D} (h\gamma_\nu^- H) \times \nu + i\kappa h \gamma_T^- E \right)
\end{aligned} \tag{17}$$

Using the scaling matrix \mathbf{S} from Section 2, we abbreviate these conditions as

$$\begin{bmatrix} \gamma_t^+ E' \\ \gamma_N^+ E' \end{bmatrix} - \mathbf{S} \begin{bmatrix} \gamma_t^- E' \\ \gamma_N^- E' \end{bmatrix} = - \begin{bmatrix} F_1^+ \\ F_2^+ \end{bmatrix} + \mathbf{S} \begin{bmatrix} F_1^- \\ F_2^- \end{bmatrix}. \tag{18}$$

Arguing as in the derivation of (12), we obtain the system of integral equations

$$\left(\mathbf{S} \mathbf{A}_\kappa \mathbf{S}^{-1} + \mathbf{A}_{k_0} \right) \begin{bmatrix} \gamma_t^+ E' \\ \gamma_N^+ E' \end{bmatrix} = \left(\frac{1}{2} \mathbf{I} - \mathbf{S} \mathbf{A}_\kappa \mathbf{S}^{-1} \right) \begin{bmatrix} F_1^+ \\ F_2^+ \end{bmatrix} + \mathbf{S} \left(\mathbf{A}_\kappa - \frac{1}{2} \mathbf{I} \right) \begin{bmatrix} F_1^- \\ F_2^- \end{bmatrix} \tag{19}$$

Note that (19) differs from (12) only in the right hand side, i.e. the same solver can be used to compute E and E' .

For a perfectly conducting obstacle, the derivation of E' follows along the same lines. The final result is that $E' \in H(\text{curl}, B \setminus \overline{D})$ is a solution of (7) for $E^i = 0$ together with the boundary condition

$$\gamma_t E' = -\nabla_{\partial D} [h\gamma_\nu E] \times \nu + ik_0 h \gamma_T H.$$

The corresponding boundary integral equation is

$$\mathbf{E}_{k_0} \varphi = \nabla_{\partial D} [h\gamma_\nu E] \times \nu - ik_0 h \gamma_T H \quad \text{on } \partial D, \tag{20}$$

which again is an equation with the same integral operator as in (9).

4 Discretization of the Newton scheme

As mentioned above, the derivation of the Newton scheme requires that the set \mathcal{Y} of admissible boundaries is an open subset of a normed space. Thus, let \mathcal{Y} be the set of smooth starlike domains with center in the origin. The boundaries can then be identified by positive functions on the unit sphere \mathbb{S}^2 via spherical coordinates, i.e.

$$\partial D = \{x \in \mathbb{R}^3 : x = r(d)d, \quad d \in \mathbb{S}^2\}$$

for some smooth $r : \mathbb{S}^2 \rightarrow \mathbb{R}_{>0}$. To be more precise, we choose the open set

$$\mathcal{Y} = \{r \in C^\infty(\mathbb{S}^2) : r(d) > 0, \quad d \in \mathbb{S}^2\}$$

in the normed space $\mathcal{X} = C^\infty(\mathbb{S}^2)$ as domain for the boundary-to-far-field operator \mathbf{F} .

There are two straight forward possibilities to discretize (16). One can discretize the full Tikhonov operator $\mathbf{F}'[\partial D]^* \mathbf{F}'[\partial D] + \alpha \mathbf{I}$ or one can discretize every operator involved and

multiply them on the discrete level. In general, one expects differences in the results. Here, we choose the second idea.

We start by discretizing \mathcal{X} . Let Y_n^m , $n \in \mathbb{N}_0$, $|m| \leq n$ denote the normalized spherical surface harmonics, i.e. eigenfunctions of the Laplace-Beltrami Operator $\Delta_{\mathbb{S}^2}$ with eigenvalue $-n(n+1)$

$$\Delta_{\mathbb{S}^2} Y_n^m + n(n+1)Y_n^m = 0,$$

explicitly given in spherical coordinates $(x, y, z)^\top = (\cos \varphi \sin \theta, \sin \varphi \sin \theta, \cos \varphi)^\top \in \mathbb{R}^3$ by

$$Y_n^m(\theta, \varphi) := \sqrt{\frac{(2n+1)(n-|m|)!}{4\pi(n+|m|)!}} P_n^{|m|}(\cos \theta) e^{im\varphi}, \quad \varphi \in (0, 2\pi), \theta \in (0, \pi)$$

with the associated Legendre functions P_n^m , $n \in \mathbb{N}_0$, $m \leq n$. The functions Y_n^m form an orthonormal system in $L^2(\mathbb{S}^2, \mathbb{C})$. Since we are looking for real-valued functions, we choose as discretization of \mathcal{X} the finite dimensional subspace \mathcal{X}_N , given by

$$\mathcal{X}_N := \{r \in C^\infty(\mathbb{S}^2) : r = \sum_{n=0}^N \sum_{m=0}^n \alpha_n^m \operatorname{Re} Y_n^m + \sum_{n=1}^N \sum_{m=1}^n \beta_n^m \operatorname{Im} Y_n^m\},$$

which leads to the set of admissible boundaries \mathcal{Y}_N , given by functions $r \in \mathcal{X}_N$ with $r > 0$.

We furthermore pick $M \in \mathbb{N}$ evaluation points $\hat{x}_1, \dots, \hat{x}_M \in \mathbb{S}^2$ for the far fields. Now, equation (13) reads as

$$\mathbf{F}(\alpha, \beta) = (E^\infty(\hat{x}_1), \dots, E^\infty(\hat{x}_M)) \in \mathbb{C}^{3 \times M},$$

where α and β denote the vectors of coefficients α_n^m , $n \leq N$, $m \leq n$ and β_n^m , $n \leq N$, $1 \leq m \leq n$. Using the linearity of the domain derivative, we can write

$$\mathbf{F}'[\partial D]\eta = \sum_{n=0}^N \sum_{m=0}^n \alpha_n^m \mathbf{F}'[\partial D](\operatorname{Re} Y_n^m) + \sum_{n=1}^N \sum_{m=1}^n \beta_n^m \mathbf{F}'[\partial D](\operatorname{Im} Y_n^m). \quad (21)$$

Again, using only finitely many evaluation points we have for fixed n and m :

$$\begin{aligned} \mathbf{F}'[\partial D](\operatorname{Re} Y_n^m) &= (E'_\infty(\hat{x}_1; \operatorname{Re} Y_n^m), \dots, E'_\infty(\hat{x}_2; \operatorname{Re} Y_n^m)) \in \mathbb{C}^{3 \times M}, \\ \mathbf{F}'[\partial D](\operatorname{Im} Y_n^m) &= (E'_\infty(\hat{x}_1; \operatorname{Im} Y_n^m), \dots, E'_\infty(\hat{x}_2; \operatorname{Im} Y_n^m)) \in \mathbb{C}^{3 \times M}, \end{aligned}$$

where $E'_\infty(\hat{x}; \eta)$ denotes the far field of the domain derivative E' with respect to the perturbation η , evaluated at $\hat{x} \in \mathbb{S}^2$. Choosing the ordered basis \mathcal{B} of \mathcal{Y}_N , given by

$$\mathcal{B} = \{\operatorname{Re} Y_0^0, \operatorname{Re} Y_1^0, \operatorname{Re} Y_1^1, \dots, \operatorname{Re} Y_N^N, \operatorname{Im} Y_1^1, \operatorname{Im} Y_2^1, \dots, \operatorname{Im} Y_N^N\},$$

we arrive at the representation matrices

$$\begin{aligned} \mathbf{F}'[\partial D] : \mathbb{R}^{(N+1)^2} &\rightarrow \mathbb{C}^{3 \times M} \\ (\mathbf{F}'[\partial D])_{ijk} &= (E'_\infty(\hat{x}_j; \eta_k))_i, \quad i = 1, 2, 3, j = 1, \dots, M, k = 1, \dots, (N+1)^2, \end{aligned}$$

where η_k denotes the k -th element of \mathcal{B} . The product of $\mathbf{F}'[\partial D]^* \mathbf{F}'[\partial D]$ is a complex quadratic $(N+1)^2 \times (N+1)^2$ matrix, given by

$$(\mathbf{F}'[\partial D]^* \mathbf{F}'[\partial D])_{ij} = \sum_{k=1}^M \overline{E'_\infty(x_k; \eta_i)} \cdot E'_\infty(x_k; \eta_j) \in \mathbb{C}. \quad (22)$$

Note, that the adjoint of the discrete $\mathbf{F}'[\partial D]$ is just given by complex conjugation. Similarly, if we denote by $E^\infty(\hat{x}, \partial D)$ the far field with respect to ∂D , evaluated in $\hat{x} \in \mathbb{S}^2$ the right hand side of equation (16) is an element of $\mathbb{C}^{(N+1)^2}$, given by

$$(\mathbf{F}'[\partial D]^*(E^\infty - \mathbf{F}(\partial D)))_k = \sum_{j=1}^M \overline{E'_\infty(\hat{x}_j, \eta_k)} \cdot (E^\infty(\hat{x}_j) - E^\infty(\hat{x}_j, \partial D)), \quad k = 1, \dots, (N+1)^2.$$

Instead of the the identity \mathbf{I} , we choose the diagonal penalty matrix \mathbf{J} , given by $(\mathbf{J})_{kk} = 1 + \lambda(k)$, $k = 1, \dots, (N+1)^2$. Here

$$\lambda(k) := n(n+1), \quad \text{such that } \eta_k = \operatorname{Re} Y_n^m \text{ or } \operatorname{Im} Y_n^m.$$

This corresponds to an $H^2(\mathbb{S}^2)$ -penalty, since the $H^2(\mathbb{S}^2)$ -norm is equivalent to the graph norm $\|\cdot\|_{\Delta_{\mathbb{S}^2}}$ of the Laplace-Beltrami Operator $\Delta_{\mathbb{S}^2}$, given by

$$\|\cdot\|_{\Delta_{\mathbb{S}^2}} = \|\cdot\|_{L^2(\mathbb{S}^2)} + \|\Delta_{\mathbb{S}^2} \cdot\|_{L^2(\mathbb{S}^2)}$$

and since the basis elements $\eta \in \mathcal{B}$ are eigenfunctions of $\Delta_{\mathbb{S}^2}$. So, solving the Tikhonov equation (16) after discretization of \mathcal{Y} becomes solving a linear system of $(N+1)^2$ equations.

The solution $\eta = (\alpha_0^0, \alpha_1^0, \dots, \alpha_N^N, \beta_1^1, \beta_2^1, \dots, \beta_N^N) \in \mathbb{C}^{(N+1)^2}$ of the discrete system

$$(\mathbf{F}'[\partial D]^* \mathbf{F}'[\partial D] + \alpha \mathbf{J}) \eta = \mathbf{F}'[\partial D]^*(E^\infty - \mathbf{F}(\partial D)) \quad (23)$$

is in general complex-valued. For the update in (iv), we discard the imaginary part.

The full discretization of equation (23) follows by numerically evaluating \mathbf{F} for a boundary ∂D of a given scatterer D and by evaluation of the far field of the domain derivative for a given perturbation η . We realized this with the help of the boundary element software Bempp.

5 Implementation remarks

The actual implementation of the Newton scheme requires the solution of many integral equations (9), (12), (19) or (20). The library Bempp (<https://bempp.com/>) provides a sophisticated basis for such calculations. For an introduction on how to solve electromagnetic scattering problems with Bempp, we refer to the overview paper [16] for the case of the perfect conductor and to the commented Jupyter Notebook on *Electromagnetic scattering from multiple dielectric spheres* available on the Bempp homepage (<https://bempp.com/documentation>).

The application of Bempp is particularly attractive for mathematicians as the formulation of discrete problems is exactly analogous to the corresponding full mathematical problem. Thus, in this section, we will only write down equations for the full problem, in the Sobolev space $H(\operatorname{curl}, D)$ or its trace spaces. Once it is known how to discretize each operator, the corresponding equations in the boundary element spaces are exactly the same.

As mentioned before, the boundary integral equations for the domain derivatives (19) and (20) differ only in the right hand side from the boundary integral equations for the scattering problems (9) and (12), respectively. Let us recall the right hand sides for the perfect conductor

$$F := \nabla_{\partial D}[h\gamma_\nu(E)] \times \nu - ik_0\gamma_\nu h\gamma_T H \quad (24)$$

and for the penetrable scatterer

$$\left(\frac{1}{2}\mathbf{I} - \mathbf{S}\mathbf{A}_\kappa\mathbf{S}^{-1}\right) \begin{bmatrix} F_1^+ \\ F_2^+ \end{bmatrix} + \mathbf{S} \left(\mathbf{A}_\kappa - \frac{1}{2}\mathbf{I}\right) \begin{bmatrix} F_1^- \\ F_2^- \end{bmatrix}$$

with

$$\begin{bmatrix} F_1^+ \\ F_1^- \\ F_2^+ \\ F_2^- \end{bmatrix} := \begin{bmatrix} \nabla_{\partial D}(h\gamma_\nu^+ E) \times \nu - ik_0 h\gamma_T^+ H \\ \nabla_{\partial D}(h\gamma_\nu^- E) \times \nu - i\kappa h\gamma_T^- H \\ \nabla_{\partial D}(h\gamma_\nu^+ H) \times \nu + ik_0 h\gamma_T^+ E \\ \nabla_{\partial D}(h\gamma_\nu^- H) \times \nu + i\kappa h\gamma_T^- E \end{bmatrix}. \quad (25)$$

This leads to the following tasks:

1. Calculation of the normal traces γ_ν^\pm of E and H .
2. Calculation of the product of h and the traces of E and H .
3. Calculation of the surface gradient of these products.
4. Rotation of the surface gradient and calculation of the trace γ_T of E and H .

By solving the direct scattering problem, we gain access to φ , the solution of

$$\gamma_t^+ E^i = \mathbf{E}_{k_0} \varphi, \quad \text{on } \partial D$$

in the case of the perfect conductor and to $(\gamma_t^+ E^s, \gamma_N^+ E^s)$ in the case of the penetrable scatterer.

We use

$$\text{Div}_{\partial D}(\gamma_t w) = \gamma_\nu \text{curl } w, \quad w \in H(\text{curl}, D), \quad (26)$$

see [2], the corresponding equation for $w \in H(\text{curl}, B \setminus \bar{D})$ and Maxwell's equations to obtain the relations

$$\begin{bmatrix} \gamma_\nu^+ k_0 E \\ \gamma_\nu^- \kappa E \end{bmatrix} = -\frac{1}{i} \text{Div}_{\partial D} \begin{bmatrix} \gamma_N^+ E \\ \gamma_N^- E \end{bmatrix}, \quad \begin{bmatrix} \gamma_\nu^+ k_0 H \\ \gamma_\nu^- \kappa H \end{bmatrix} = \frac{1}{i} \text{Div}_{\partial D} \begin{bmatrix} \gamma_t^+ E \\ \gamma_t^- E \end{bmatrix}.$$

For the case of a penetrable scatterer, we arrive at explicit formulas for the normal traces. In the case of the perfect conductor, we can calculate the unknown Neumann trace $\gamma_N E$ with the help of the jump conditions. If φ is the solution of the EFIE (9), i.e. $E^s = -\mathcal{E}_{k_0} \varphi$, we have

$$\gamma_N E^s = -\gamma_N \mathcal{E}_{k_0} \varphi = \left(\frac{1}{2}\mathbf{I} - \mathbf{H}_{k_0}\right) \varphi.$$

Again using (26), we obtain normal traces using the surface divergence $\text{Div}_{\partial D}$. One can see from (6) that the weak formulations for the surface divergence and the surface gradient are coupled. Assuming further smoothness, we can write:

$$\int_{\partial D} \psi \text{Div}_{\partial D} \varphi \, ds = - \int_{\partial D} \varphi \cdot \nabla_{\partial D} \psi \, ds$$

Up to the sign, the left hand side can be seen as weak formulation of the surface gradient and the right hand side as weak formulation of the surface divergence. Bempp supports the weak formulation of a number of surface differential operators. The details of the implementation

are documented in a Jupyter notebook associated with this paper available through the Bempp homepage (<https://bempp.com/publications>).

In order to calculate the product of two discrete functions f and g and represent the result in a given basis $\{\phi_j\}$ we solve the linear system of equations

$$\sum_i \alpha_i \int_{\partial D} \phi_i(x) \phi_j(x) ds = \int_{\partial D} \phi_j(x) \cdot (f(x)g(x)) ds, \quad j = 1, \dots$$

to obtain the L^2 projection of the function product on the basis $\{\phi_j\}$. Here, depending on whether the product is scalar (in the case of $\gamma_\nu h \gamma_\nu E$), or vectorial (in the case of $\gamma_\nu h \gamma_T E$) we choose the basis $\{\phi_j\}$ to be either scalar or vectorial.

So far, we have explained, how we can fulfill tasks 1. - 3. The remaining task is the rotation of the surface gradient $\nabla_{\partial D} \times \nu$ and the calculation of the traces γ_T of E and H . Since the two traces γ_t and γ_T are formally connected to each other by rotation:

$$\gamma_T \phi = \nu \times (\phi \times \nu) = -(\phi \times \nu) \times \nu = -\gamma_t \phi \times \nu,$$

we only need to implement the rotation. Considering

$$\begin{aligned} \int_{\partial D} \gamma_T \varphi \cdot \gamma_t \psi ds &= \int_{\partial D} (\nu \times (\varphi \times \nu)) \cdot (\psi \times \nu) ds = \int_{\partial D} \varphi \cdot (\psi \times \nu) ds \\ &= - \int_{\partial D} \psi \cdot (\varphi \times \nu) ds = - \int_{\partial D} (\nu \times (\psi \times \nu)) \cdot (\varphi \times \nu) ds = - \int_{\partial D} \gamma_t \varphi \cdot \gamma_T \psi ds, \end{aligned}$$

we observe that $\langle \cdot, \cdot \rangle_{\partial D}$ can be seen as weak formulation for the operator R with $R\gamma_T \varphi = \gamma_t \varphi$ and $-\langle \cdot, \cdot \rangle_{\partial D}$ for the converse operator. Again, Bempp provides the tools to implement this as demonstrated in the associated Jupyter notebook available at <https://bempp.com/publications>. Observe that for every tangential vector field φ , we have $(\nu \times (\varphi \times \nu)) = \varphi$. Therefore, rotating the surface gradient of φ can be seen as applying Λ , i.e. $(\nabla_{\partial D} \varphi) \times \nu = \Lambda(\nabla_{\partial D} \varphi)$.

6 Numerical results

In this section we present the results of some of the numerical experiments we have carried out.

We have successfully run reconstructions for the perfect conductor and for the penetrable scatterer. In both cases we have considered exact and noisy data. Below, we present the results for the penetrable scatterer. Results for the perfect conductor are similar, but require less computational effort.

In order to test our implementation of the reconstruction algorithm, we have picked the following shapes, see figure 1:

1. A rounded cuboid, implicitly given by

$$(x_1/r_1)^n + (x_2/r_2)^n + (x_3/r_3)^n = d^n$$

with some exponent $n \in \mathbb{N}$, positive radius d and side lengths $r_1, r_2, r_3 > 0$.

2. A peanut shaped object, implicitly given by

$$\left(\frac{x_1}{R(\frac{2}{d}x_3)}\right)^2 + \left(\frac{x_2}{R(\frac{2}{d}x_3)}\right)^2 + x_3^2 = \frac{d^2}{4},$$

with $R : [-1, 1] \rightarrow \mathbb{R}$, $R(z) = \frac{3}{5} - \frac{2}{5} \cos\left(\frac{\pi}{2}z\right)$.

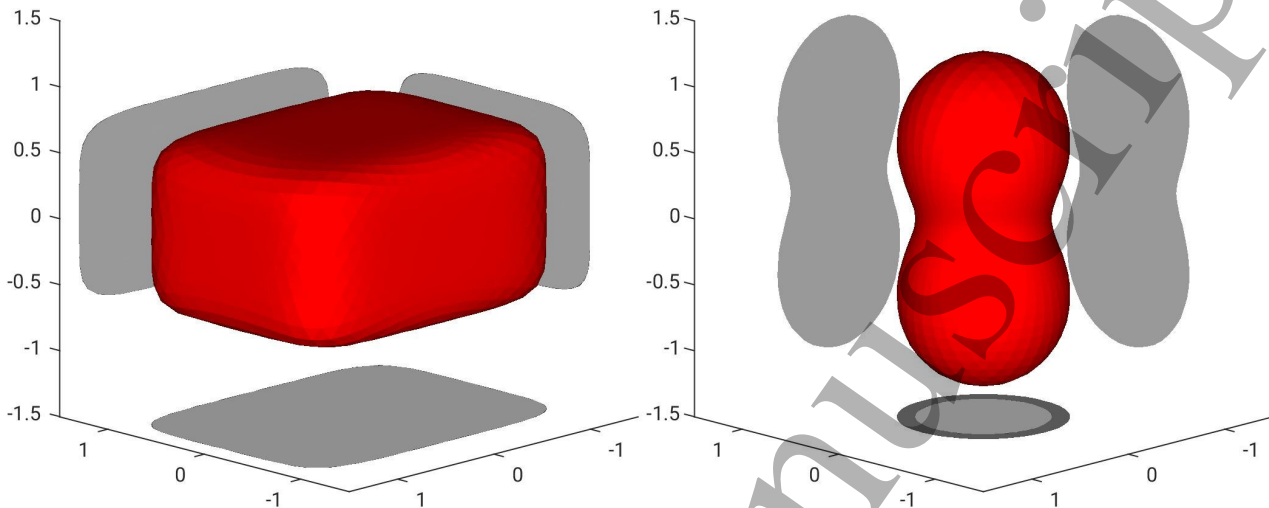


Figure 1: The rounded cuboid with $n = 6$ and $(r_1, r_2, r_3) = (1, 1.3, 0.7)$ and $d = 1$ on the left and the peanut with $d = 2.5$ on the right.

We chose the first object in order to have an object close to the non-smooth cuboid. Of course, the actual rounded cuboid is smooth for every $n \in \mathbb{N}$, but does not lie in the span of our shape basis functions. Our implementation requires starlike shaped objects, but no convexity. Therefore we picked the second object as an example for a non convex object. To cancel positive effects due to symmetry, we applied a translation such that the center of the two starlike objects does not coincide with the center of our starlike reconstruction in 0.

First, we generated the exact data $E_\infty = \mathbf{F}(\partial D)$. We have picked 168 evaluation points \hat{x}_i , $i = 1, \dots, 168$ on the unit sphere \mathbb{S}^2 , so that the discrete version of E_∞ is an element of $\mathbb{C}^{3 \times 168}$. In order to avoid an inverse crime, we ran calculations of the exact data with meshes unrelated to those used in the reconstruction and yielding a higher accuracy. In the case of noisy data, we multiplied every component of $E_\infty \in \mathbb{C}^{3 \times 168}$ with some perturbation factor of the form

$$1 + \delta \lambda_1 e^{2\pi i \lambda_2},$$

where λ_1, λ_2 are on $(0, 1)$ uniformly distributed random numbers and the noise level $\delta \geq 0$. We call this *noise up to* δ . The effective noise level is given by

$$\delta_{\text{eff}} = \frac{\|E_\infty - E_\infty^\delta\|}{\|E_\infty\|}. \quad (27)$$

Since the noisy far field E_∞^δ is no longer a (discrete) tangential vector field on the sphere, one might think of cancelling the non tangential parts of E_∞^δ , but since we apply the adjoint of $\mathbf{F}[\partial D_i]$ on the right hand side of (16), non tangential parts get canceled automatically. For the

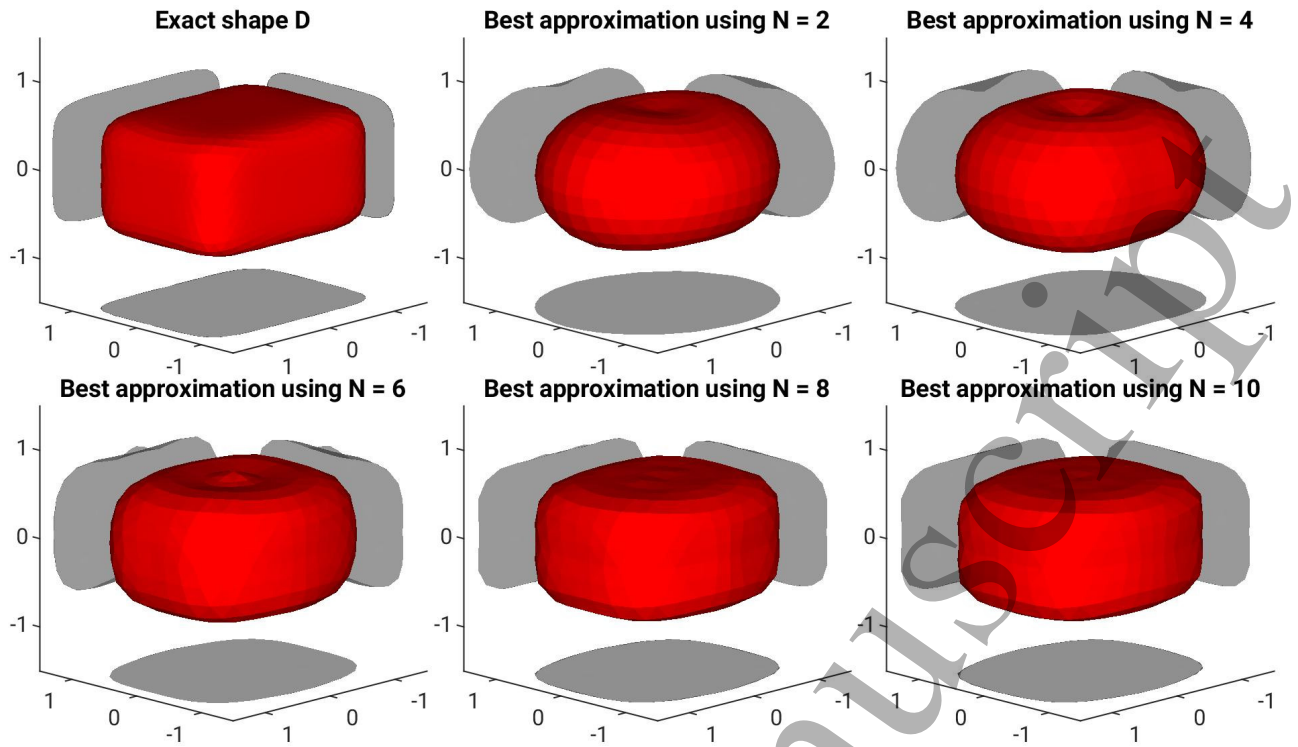


Figure 2: The best approximation of the rounded cuboid using $(N + 1)^2$ basis elements.

calculation of δ_{eff} , we did not see any relevant difference, if we just considered the tangential part of E_{∞}^{δ} in (27).

As initial guess, we have chosen $D_0 = B_1(0) = \{x \in \mathbb{R}^3, \|x\| \leq 1\}$, the ball of radius one. We have observed that we have to either increase the regularization parameter α drastically or use some a-priori information about the size of the scatterer for successful reconstructions.

We have chosen the regularization parameter α by experience. Using too small parameters, especially in the case of noisy data, leads to updates of the parameterization, where negative radii occur, i.e. degenerated objects. But above some critical level, we have observed robust reconstructions. Using larger than necessary α slows down the reconstruction speed, but the effect is barely noticeable. In the case of exact data, we have used $\alpha = 3$ and for noisy data $\alpha = 7$ for the peanut and $\alpha = 12$ for the rounded cuboid, which seems to be necessary for reasonable noise levels. Reconstructions with lower values of α have failed from time to time.

Choosing a fixed number of basis elements for the construction, one can calculate the $L^2(\mathbb{S}^2)$ projection of the parameterization onto these elements. The resulting shapes are in this sense the best reconstructions, one can hope for. In Figure 2, one can see the best approximation of the rounded cuboid using different numbers of basis elements.

For our reconstructions, we have chosen the material parameters

$$\varepsilon_r = 2.1, \quad \mu_r = 1.0, \quad k_0 = 1.0472, \quad \kappa = 1.5175,$$

which correspond to the scattering of Teflon (C_2F_4) illuminated by VHF radiation with wavelength of 6 m.

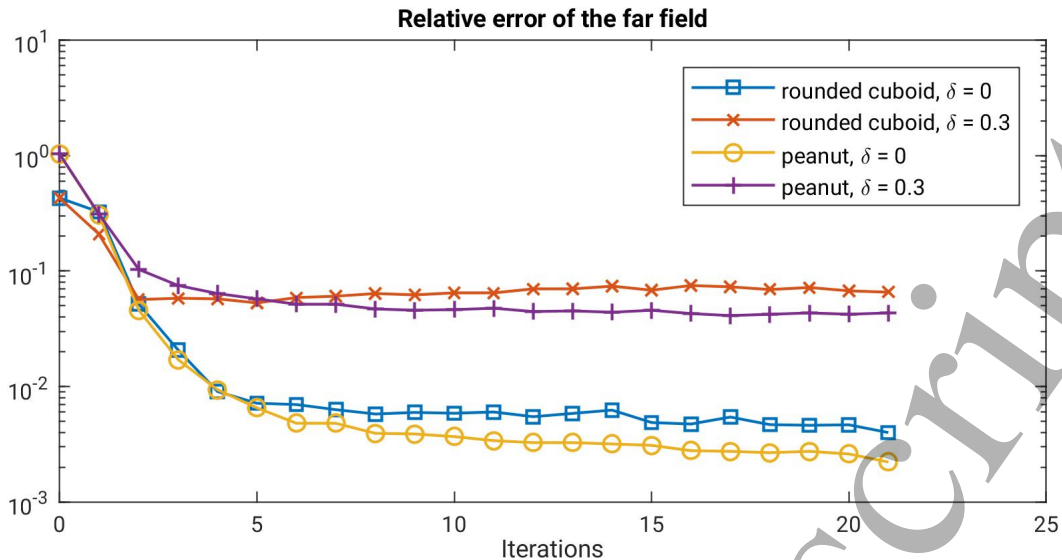


Figure 3: Residuals $\|E^\infty - \mathbf{F}(\partial D_i)\|$ during the reconstructions of the peanut and the rounded cuboid with and without noise.

We have considered one incoming pair of plane waves (E^i, H^i) , given by

$$\begin{pmatrix} E^i \\ H^i \end{pmatrix} (x) = \begin{pmatrix} p \\ (d \times p) \end{pmatrix} e^{ik_0 d \cdot x}, \quad x \in \mathbb{R}^3,$$

with polarization $p \in \mathbb{C}^3$ and direction $d \in \mathbb{S}^2$, satisfying $p \cdot d = 0$. Again, to avoid any positive effects due to symmetry, we have chosen

$$p = \begin{pmatrix} 1+i \\ 2 \\ -1 + \frac{1}{3}i \end{pmatrix} \quad \text{and} \quad d = \frac{1}{\sqrt{14}} \begin{pmatrix} 1 \\ 2 \\ 3 \end{pmatrix}.$$

Let us present our reconstructions. In all cases, we have run 21 iterations without stopping rule. We have chosen $N = 7$, i.e. we have used $(N + 1)^2 = 64$ basis functions. In Figure 3, the normalized residuals

$$e_i := \frac{\|E^\infty - \mathbf{F}(\partial D_i)\|}{\|E^\infty\|}$$

are plotted for the reconstruction of the peanut and the rounded cuboid with and without noise. Note the relatively large initial error e_0 with $e_0 \approx 0.4$ for the rounded cuboid and $e_0 \approx 1.0$ for the peanut. Also observe that after some iterations, the residuals stay at the same level. For noise free data, we have achieved final errors of $e_{21} \approx 2 \cdot 10^{-3}$ for the peanut and $e_{21} \approx 4 \cdot 10^{-3}$ for the rounded cuboid. Considering noisy data, we achieved $e_{21} = 4 \cdot 10^{-2}$ for the peanut and $e_{21} = 6.5 \cdot 10^{-2}$ for the rounded cuboid.

In Figures 4, 5, 6 and 7 reconstructions of the peanut and the rounded cuboid, each with exact and noisy data are represented. The arrow in the picture with the exact shape D indicates the direction d of the incoming plane wave. Observe the indentation of the reconstruction of the peanut along d even for noise free data, which is a known phenomena for acoustic scattering problems.

1
2
3 We have applied noise up to $\delta = 0.3$, which lead to the effective noise level $\delta_{\text{eff}} \approx 0.13$ for the
4 rounded cuboid and $\delta_{\text{eff}} \approx 0.12$ for the peanut.

5
6 For our calculation, we have used machines with 32 or 64 CPU cores. With the help of some
7 parallelization, we have been able to run one iteration of our algorithm in about 10 to 20
8 minutes.
9

10 In conclusion, we have shown how iterative regularization schemes that have been used in
11 inverse acoustic scattering problems for some time, can also be implemented and applied to
12 electromagnetic scattering problems. The results of the numerical experiments have been
13 obtained with a reasonable computational effort and are very promising. In particular, the
14 reconstructions appear to be of better quality than those obtained for acoustic scattering in
15 [7]. We believe that this is due to the vectorial as opposed to scalar nature of the fields which
16 provides additional information for the reconstruction. Hence, Newton type schemes may be
17 particularly attractive for inverse electromagnetic scattering problems.
18
19
20

21 Acknowledgements

22
23
24 We gratefully acknowledge financial support by the Deutsche Forschungsgemeinschaft (DFG)
25 through CRC 1173.
26
27
28
29
30
31
32
33
34
35
36
37
38
39
40
41
42
43
44
45
46
47
48
49
50
51
52
53
54
55
56
57
58
59
60

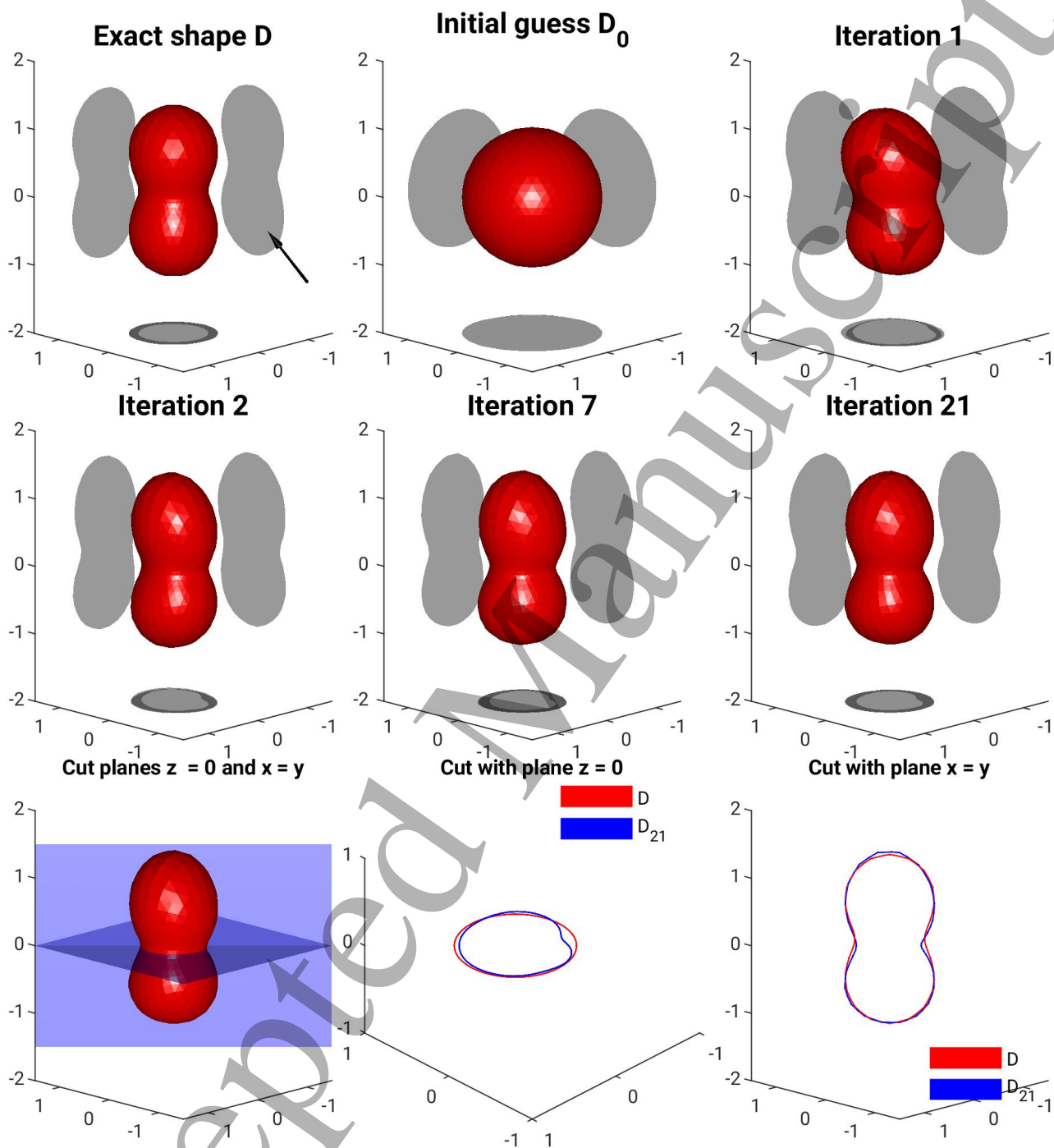


Figure 4: Reconstruction of the Peanut without noise.

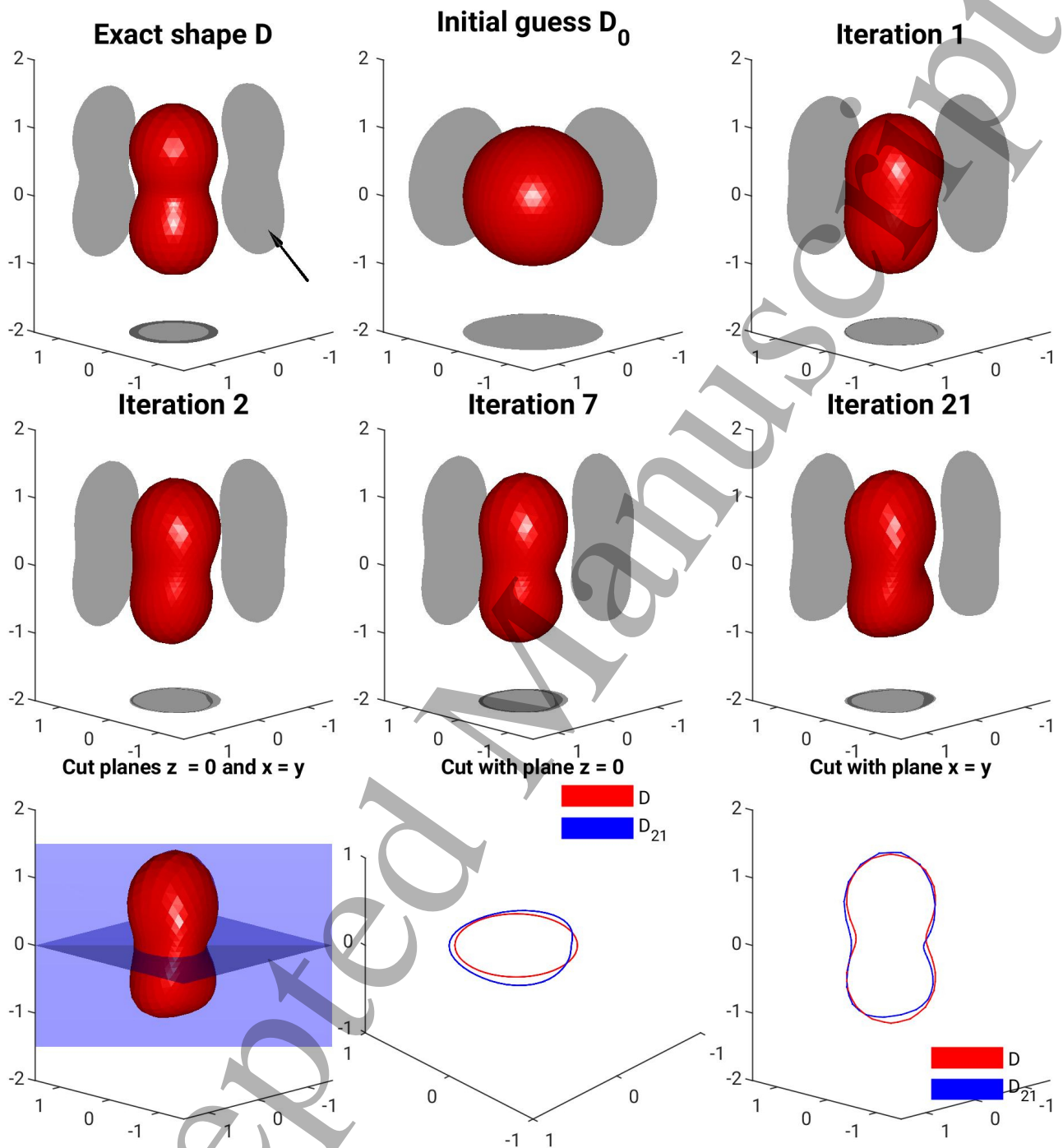


Figure 5: Reconstruction of the Peanut with up to 30% noise.

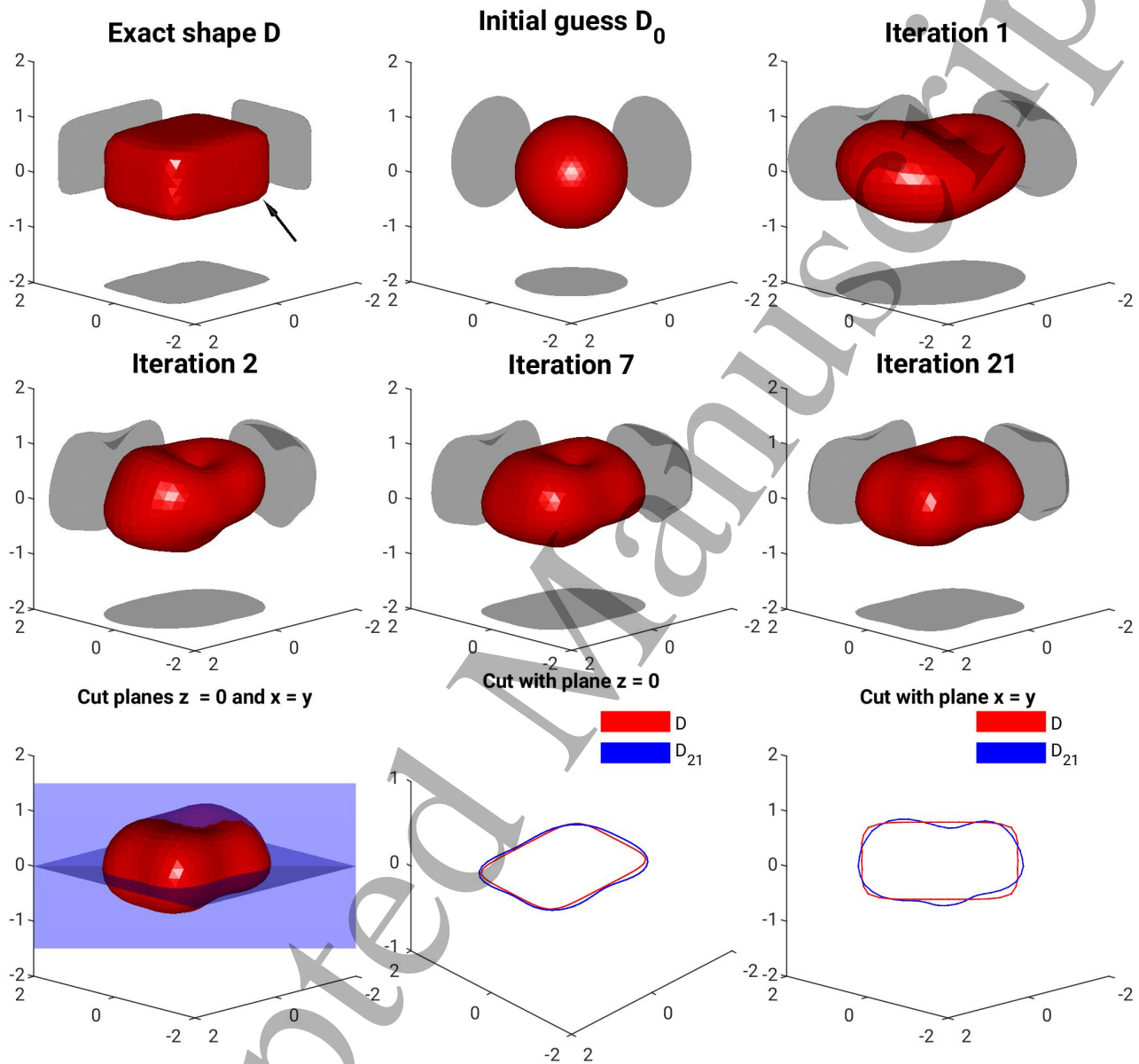


Figure 6: Reconstruction of the rounded cuboid without noise.

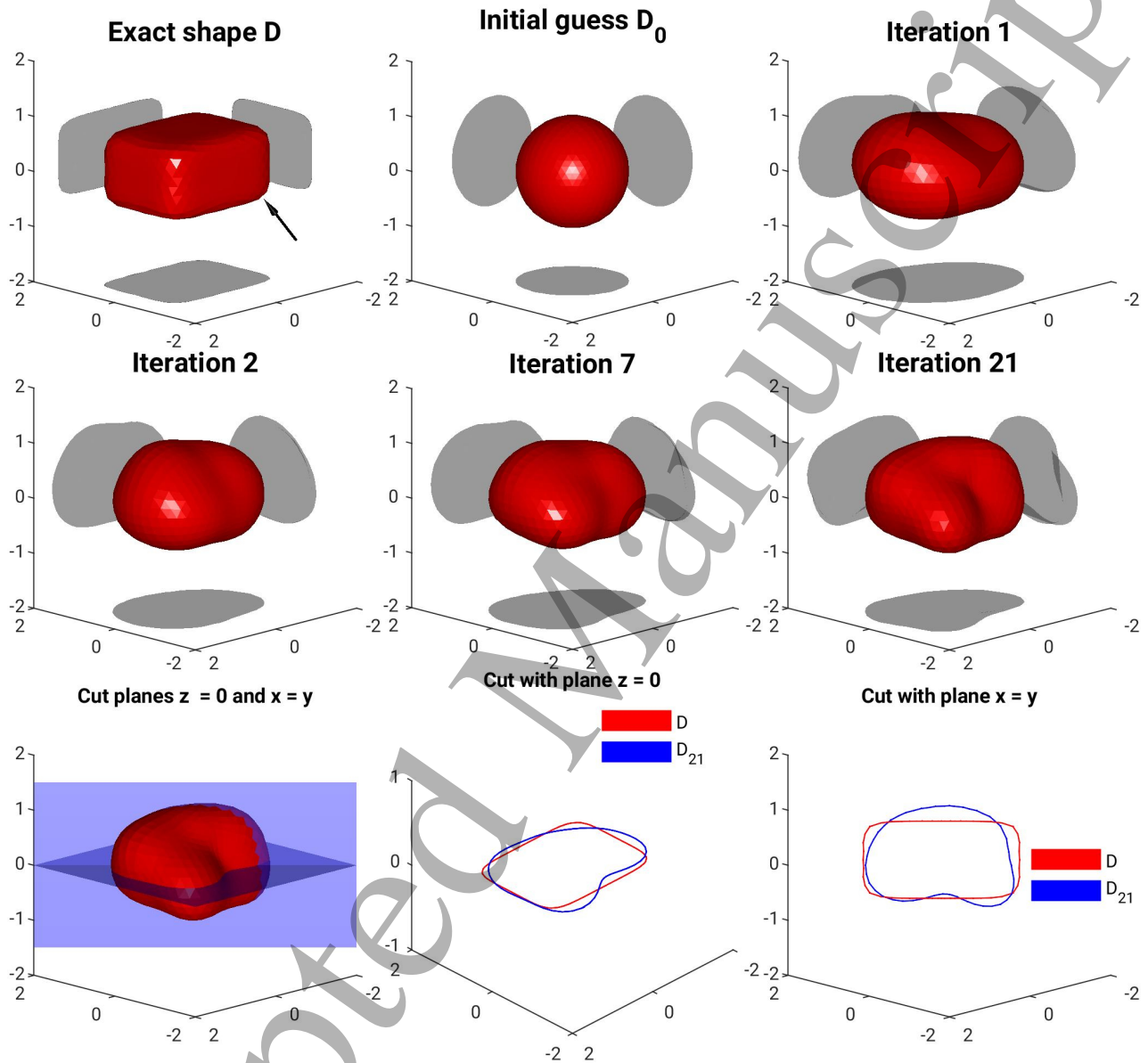


Figure 7: Reconstruction of the rounded cuboid with up to 30% noise.

References

- [1] T. Abboud and J.C. Nédélec. Electromagnetic waves in an inhomogeneous medium. *J. Math. Anal. Appl.*, 164:40–58, 1992.
- [2] A. Buffa, M. Costabel, and D. Sheen. On traces for $H(\text{curl}, \Omega)$ in Lipschitz domains. *J. Math. Anal. Appl.*, 276:845–867, 2001.
- [3] A. Buffa and R. Hiptmair. Galerkin boundary element methods for electromagnetic scattering. In M. Ainsworth, P. Davies, D. Duncan, P. Martin, and B. Rynne, editors, *Topics in Computational Wave Propagation, Direct and Inverse Problems*, volume 31 of *Lecture Notes in Computational Science and Engineering*, pages 83–124. Springer, Berlin, 2003.
- [4] A. Buffa, R. Hiptmair, T. von Petersdorff, and C. Schwab. Boundary element methods for Maxwell transmission problems in Lipschitz domains. *Numerische Mathematik*, 95(3):459–485, 2003.
- [5] D. Colton and R. Kress. *Inverse Acoustic and Electromagnetic Scattering Theory*. Springer, New York, 3rd edn. edition, 2013.
- [6] M. Costabel and F. Le Louër. Shape derivatives of boundary integral operators in electromagnetic scattering. Part I: Shape differentiability of pseudo-homogeneous boundary integral operators. *Integral Equations and Operator Theory*, 72:509–535, 2012.
- [7] Helmut Harbrecht and Thorsten Hohage. Fast methods for three-dimensional inverse obstacle scattering problem. *Integral Equations and Applications*, 19:237–260, 2007.
- [8] F. Hettlich. *The Domain Derivative in Inverse Obstacle Problems*. Habilitation Thesis, University of Erlangen, Erlangen, 1999.
- [9] F. Hettlich. The domain derivative of time-harmonic electromagnetic waves at interfaces. *Math. Meth. Appl. Sci.*, 35:1681–1689, 2012.
- [10] R. Hiptmair and J. Li. Shape derivatives for scattering problems. *Inverse Problems*, 34:105001 (25pp), 2018.
- [11] B. Kaltenbacher, A. Neubauer, and O. Scherzer. *Iterative Regularization Methods for Nonlinear Ill-Posed Problems*. de Gruyter, Berlin, 2008.
- [12] A. Kirsch and F. Hettlich. *The Mathematical Theory of Time-Harmonic Maxwell’s Equations*. Springer, 2015.
- [13] R. Kress. Electromagnetic waves scattering: Scattering by obstacles. In E. Pike and P. Sabatier, editors, *Scattering*, pages 191–210. Academic Press, London, 2001.
- [14] P. Monk. *Finite Element Methods for Maxwell’s Equations*. Oxford Science Publications, Oxford, 2003.
- [15] R. Potthast. Domain derivatives in electromagnetic scattering. *Math. Meth. Appl. Sci.*, 19:1157–1175, 1996.

- 1
2
3 [16] M.W. Scroggs, T. Betcke, E. Burman, W. Śmigaj, and E. van't Wout. Software frame-
4 works for integral equations in electromagnetic scattering based on calderón identities.
5 *Computers and Mathematics with Applications*, 74:2897–2914, 2017.
6
7 [17] W. Śmigaj, S. Arridge, T. Betcke, J. Phillips, and M. Schweiger. Solving boundary integral
8 problems with BEM++. *ACM Transactions on Mathematical Software*, 41(2):6:1–6:40,
9 2015.
10
11
12
13
14
15
16
17
18
19
20
21
22
23
24
25
26
27
28
29
30
31
32
33
34
35
36
37
38
39
40
41
42
43
44
45
46
47
48
49
50
51
52
53
54
55
56
57
58
59
60